Eur. Phys. J. D **9**, 385–388 (1999)

THE EUROPEAN PHYSICAL JOURNAL D

EDP Sciences

A molecular dynamics study on the formation of metallofullerene

Y. Yamaguchi and S. Maruyama[a]

Department of Mechanical Engineering, The University of Tokyo, 7-3-1 Hongo, Bunkyo-ku, Tokyo 113-8656, Japan

Received: 2 September 1998 / Received in final form: 3 January 1999

Abstract. The growth process of metallofullerene was studied by the use of the molecular dynamics method. Based on density functional theory (DFT) calculations of various forms of small clusters MC_n and M_n (M = La, Sc, Ni), multi-body classical potential functions for M–C and M–M interactions were constructed with the Morse term and the Coulomb term as functions of the coordinate number of a metal atom. The clustering process, starting from 500 isolated carbon atoms and 5 metal atoms, was simulated under a controlled temperature condition, $T_c = 3000$ K. When La atoms were applied, the stable open-cap structure surrounding the La atom resulted in the lanthanum-containing caged cluster. For the Sc–C system, the host carbon clusters were not affected as much as they were in the La–C case, because of the weaker Coulomb interaction. The precursor Sc atom was encapsulated in the host cage at the final stage of the growth process. For the Ni–C system, the precursor clusters were similar to those in Sc–C system, although the Ni atom finally stayed on the face of a large ring of the caged structure.

PACS. 36.40.-c Atomic and molecular clusters – 31.15.Qg Molecular dynamics and other numerical methods

1 Introduction

After the discovery of C_{60} by Kroto *et al.* [1], macroscopic amounts of empty fullerenes [2, 3], metallofullerenes [4–7], higher fullerenes [8], and carbon nanotubes [9] were successively produced and isolated. Recently, the high-quality generation of single-wall nanotubes (SWNT) [10, 11] has demonstrated new possibilities for applications of this material. Although the fullerene is now recognized as an attractive new material, the formation mechanism of these symmetric hollow-caged structures is still unknown, because the generation techniques of fullerenes [2], metallofullerenes [4], and SWNT [10] were discovered almost accidentally.

We performed molecular dynamics (MD) simulations of the clustering process of carbon atoms to investigate the fullerene formation mechanism [12, 13], and we observed the temperature dependence of the cluster structures. In addition, we demonstrated the formation of a perfect C_{60} structure by giving sufficient collision-free annealing time, and examined the time and temperature scale of the annealing process through the reaction rate of the network transformations. Based on these results, a new formation model of empty fullerenes that includes the temperature effect was proposed [13].

In this paper, the formation process of metallofullerene is studied using similar MD simulations. In spite of possible interesting applications of the metallofullerene, it is still difficult to obtain macroscopic amounts of sample because of the extremely low yield of generation. In order to find the optimum generation condition, it is imperative that we understand the formation mechanism. According to experimental studies, the metal atoms such as La, Y, Sc, (Ca), and lanthanides can be enclosed inside the carbon cage, and the preferred carbon cage structure depends on the metal. On the other hand, Ni, Co, and Fe, which are not experimentally assigned to be encapsulated in the fullerene cage, are required to generate the SWNT [10, 11]. Here, the effects of these metal atoms on the carbon cluster growth process are still unknown. In this paper, we study the differences in the growth processes among La, Sc and Ni containing systems to investigate the effect of metal atoms.

2 Method

The potential function among carbon atoms was the same as our previous reports [12–14]. For the purpose of modeling the metal– carbon and metal–metal potential function appropriate for the MD simulation, the binding energy and charge state of various forms of small clusters MC_n and M_n (M=La, Sc, Ni; $n = 1 - 3$) were calculated. Here the density functional theory based on Becke's three-parameter exchange functional [15] with the Lee–Yang–Parr correlation [16] (B3LYP) was applied with the ef-

[a] Corresponding author. Fax: +81-3/5800-6983,
e-mail: maruyama@photon.t.u-tokyo.ac.jp

Table 1. Potential parameters for metal–carbon interactions.

	D_e (eV)	S	β (1/Å)	R_e (Å)	R_1 (Å)	R_2 (Å)	b	δ	k_1	k_2
La–C	4.53	1.3	1.5	2.08	3.2	3.5	0.0854	−0.8	0.0469	1.032
Sc–C	3.82	1.3	1.7	1.80	2.7	3.0	0.0936	−0.8	0.0300	1.020
Ni–C	3.02	1.3	1.8	1.70	2.7	3.0	0.0330	−0.8	–	–

Table 2. Potential parameters for metal–metal interactions.

	S	β(1/Å)	D_{e1}(eV)	D_{e2}(eV)	C_D	R_{e1}(Å)	R_{e2}(Å)	C_R	R_1(Å)	R_2(Å)
La–La	1.3	1.05	0.740	2.64	0.570	3.735	0.777	0.459	4.0	4.5
Sc–Sc	1.3	1.4	0.645	1.77	0.534	3.251	0.919	0.620	3.5	4.0
Ni–Ni	1.3	1.55	0.74	1.423	0.365	2.520	0.304	0.200	2.7	3.2

fective core potentials derived from the LANL2DZ basis of Gaussian 94 [17]. The semi-empirical calculation results [18] were also referred to for the Ni–Ni interaction.

Metal-carbon multi-body potential functions were constructed as functions of the carbon coordinate number of a metal atom. The total potential energy is expressed as the sum of binding energy E_b as follows.

$$E_b = V_R + V_A + V_C \tag{1}$$

$$V_R = f(r_{ij})\frac{D_e}{S-1}\exp\left\{-\beta\sqrt{2S}(r_{ij}-R_e)\right\} \tag{2}$$

$$V_A = -f(r_{ij})\cdot B^*\frac{D_e S}{S-1}\exp\left\{-\beta\sqrt{2/S}(r_{ij}-R_e)\right\} \tag{3}$$

$$V_C = -f(r_{ij})\frac{e^2}{4\pi\varepsilon_0}\frac{c_C c_M}{r_{ij}} \tag{4}$$

Here, r_{ij} denotes the distance between metal i and carbon j. V_R and V_A are Morse-type repulsive and attractive terms, respectively. The Coulomb term V_C is applied only to the La–C and Sc–C interactions, which were calculated to be strongly ionic due to the electron transfer from the metal to carbon atoms.

The coordinate number of the metal atom N^C is defined using the cutoff function $f(r)$, and both the additional term B^* and electric charge c are expressed as functions of the coordinate number. Here, the effect of the angle among bonds is ignored.

$$f(r) = \begin{cases} 1 & (r < R_1) \\ \left(1+\cos\frac{r-R_1}{R_2-R_1}\right)/2 & (R_1 < r < R_2) \\ 0 & (r > R_2) \end{cases} \tag{5}$$

$$N^C = 1 + \sum_{\text{carbon } k(\neq j)} f(r_{ik}) \tag{6}$$

$$B^* = \left\{1 + b\left(N^C - 1\right)\right\}^{\delta} \tag{7}$$

$$c_M = 3 - \exp\left(-k_1 N^C + k_2\right), c_C = c_M/N^C \tag{8}$$

In (8), the limit amount of the charge transfer for a large number of carbon atoms is set to 3 in accordance with the *ab initio* calculation of isolated La@C_{82} [19]. Here, the @ denotes the encapsulation.

The potential parameters are determined as shown in Table 1. Actually, this potential is a rough estimation, because the parameterization is based on the extrapolation of DFT calculation results of only small MC_n clusters ($n = 1-3$) with some adjustments of the energy levels. It is almost impossible to calculate all the intermediate structures to determine the accurate potential function, since the number of carbon atoms varies in a wide range. Instead, this simple formulation can clarify the qualitative differences of the La–C, Sc–C and Ni–C interactions as strongly ionic, weakly ionic, or nonionic, respectively.

Metal–metal interactions were constructed in the same formula as in (1). In this case, we express the equilibrium binding energy D_e and the bond length R_e as direct functions of the metal coordinate number N_{ij}, instead of using the additional term B^* in (3).

$$N_{ij} = (N_i^M + N_j^M)/2,$$
$$N_i^M = 1 + \sum_{\text{metal}k(\neq j)} f(r_{ik}) \tag{9}$$

$$D_e(N_{ij}) = D_{e1} + D_{e2}\exp\{-C_D(N_{ij}-1)\} \tag{10}$$

$$R_e(N_{ij}) = R_{e1} - R_{e2}\exp\{-C_R(N_{ij}-1)\} \tag{11}$$

The potential parameters are shown in Table 2.

The temperature control method is also the same as in our previous report [12], where the translational, rotational, and vibrational temperatures of the system were independently controlled every 0.1 ps by simple velocity scaling so that the difference between the control temperature T_c and each individual temperature was reduced to 60%. Verlet's method was adopted for the integration of the differential equation of motion.

3 Results and discussions

3.1 Lanthanum-containing system

Five hundred carbon atoms and 5 La atoms in gas phase with random positions and velocities were distributed in a 342 Å cubic box with a full periodic boundary condition.

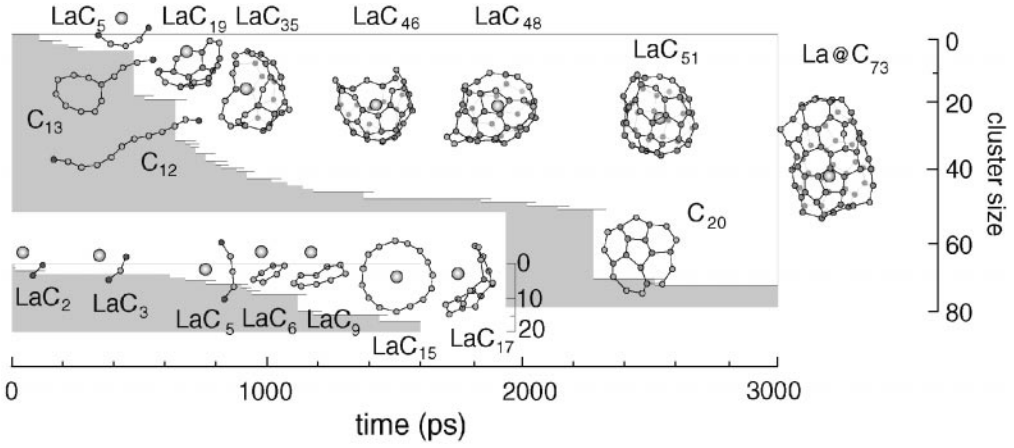

Fig. 1. Growth process of La-attached clusters (a) La@C_{73} and (b) LaC_{17}.

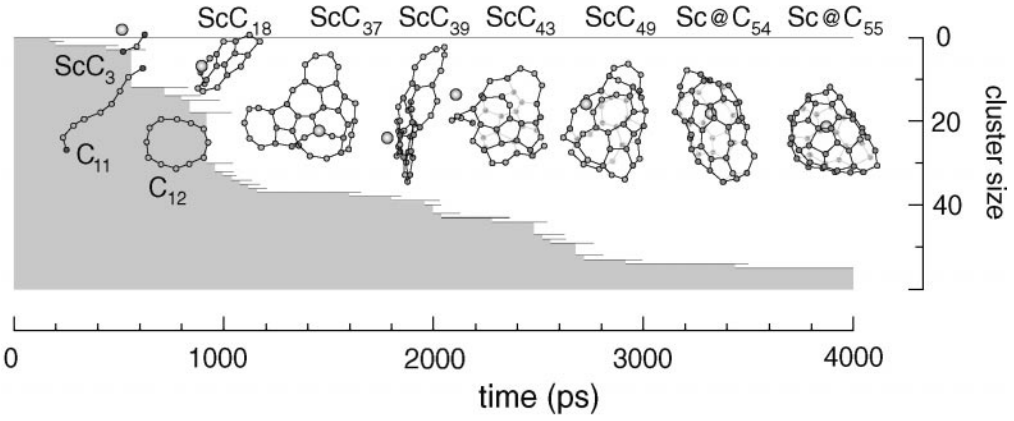

Fig. 2. Growth process of an Sc-attached cluster Sc@C_{55}.

The system was controlled toward a control temperature T_c =3000 K. These parameters correspond to the condition in which C_{60} and C_{70} caged clusters were obtained in the simulation without the inclusion of metal atoms [12].

Figure 1 shows the growth process of typical La-attached clusters in the simulation; (a) shows an La-containing caged cluster La@C_{73} observed at t =3000 ps, and (b) shows an La-attached cluster LaC_{17} observed at t =1600 ps. The vertical width and horizontal length denote the cluster size and time, respectively. For example, in Fig. 1a, it can be seen that the LaC_5 and C_{13} cluster existed independently of each other, and coalesced at about 530 ps and that the LaC_{19} was formed after the addition of a carbon atom at about 550 ps

When the cluster was smaller than LaC_5, short carbon chains surrounded the La atom (in a fan-type structure [20, 21]), as is shown in Fig. 1b. When it grew larger than LaC_6, the La atom attached to the monocyclic carbon ring, and became positioned in the center of the monocyclic ring at LaC_{15}. The host monocyclic ring changed to a polycyclic ring, and the La atom attached to it around LaC_{17}, where the Coulomb attractive force induced curvature to the host polycyclic ring. The host annealed to a curved graphitic sheet when it grew as large as LaC_{19}, as is shown in Fig. 1a, and extended the structure until about LaC_{35}, resulting in the formation of a stable open-cap structure. The cluster grew larger toward the closure of the open-cap structure; however, the number of carbon atoms was not enough to close the open-cap structure at about LaC_{50}. In this case, a collision with a large cluster of C_{20} prevented gradual growth and resulted in the formation of a caged cluster larger than La@C_{71}, and the La atom was almost encapsulated in the carbon cage. In addition, the strong Coulomb repulsion between La atoms prevented the encapsulation of two La atoms.

Considering the difference of time and temperature scale between the real phenomena and simulation [13], these hollow-caged structures could have a sufficient collision-free annealing interval to form more sophisticated structures.

3.2 Scandium-containing system

Another clustering process using Sc atoms was simulated under the same condition as in the previous section. Figure 2 shows the growth process of an Sc@C_{55} observed at $t = 4000$ ps. A remarkable difference of the process from that of the La–C system is apparent for the structures of MC_n $(20 < n < 40)$, because of the weaker Coulomb force. The cluster annealed to the 3-dimensional open cage structure around ScC_{43}, where the Sc atom moved around the open edge. The Sc atom slipped into the caged structure just before it closed, at around Sc@C_{54}.

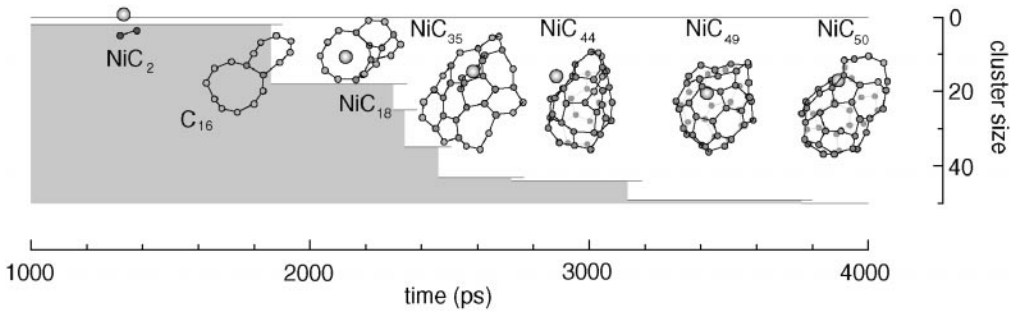

Fig. 3. Growth process of an Ni-attached cluster NiC_{50}.

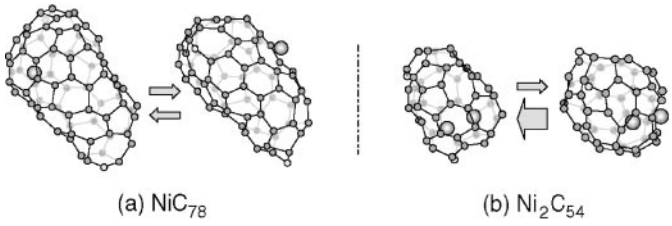

Fig. 4. Structures of Ni-attached cage clusters: (a) NiC_{78} and (b) Ni_2C_{54}.

In addition to this final stage of encapsulation, the flat structures around ScC_{35} may mean that it is possible to catch another Sc atom; this is in good agreement with the experimentally observed prominence of the dimetallofullerene for the Sc–C system.

3.3 Nickel-containing system

The nickel atom, which is not experimentally assigned to be encapsulated in the fullerene cage so far, was also examined. As shown in Fig. 3, the growth process was very similar to that for the Sc-attached cluster. However, at the final stage, the Ni atom preferred to attach at the large defect of the caged structure, e.g., large rings of more than 7 or 8 members, and frequently moved in and out of the carbon cage. Fig. 4a shows the similar behavior observed for the larger caged cluster of NiC_{78} obtained for another Ni atom.

Moreover, when two Ni atoms were enclosed in the host cage as shown in Fig. 4b, the Ni atoms remained inside the cage more stably than in the case of the single Ni atom. This result may be a hint of a new endohedral metallofullerene.

4 Conclusions

Multi-body potential functions of metal–carbon and metal–metal systems were constructed based on the DFT calculations of small MC_n and M_n (M=La, Sc, Ni) by the use of the density functional theory. When the potential function was applied to the molecular dynamics simulation, the clustering processes starting from randomly distributed carbon and metal atoms were simulated and the formation process of metal-attached caged carbon clusters were examined. When La atoms were applied, the stable open-cap structure surrounding the La atom resulted in the lanthanum-containing caged cluster. For the Sc–C system, the Sc atom was encapsulated in the host cage at the final stage of the growth process. For the Ni–C system, the Ni atom stayed on the face of a large ring of the caged structure.

This work was supported by Grant-in-Aid for JSPS Fellows (No. 08004746) and Grant-in-Aid for Scientific Research (No. 09450085) from the Ministry of Education, Science, Sports, and Culture, Japan.

References

1. H.W. Kroto *et al.*: Nature **318**, 162 (1985)
2. W. Krätschmer *et al.*: Nature **347**, 354 (1990)
3. R.E. Haufler *et al.*: Proc. Mater. Res. Soc. Symp. **206**, 627 (1991)
4. Y. Chai *et al.*: J. Phys. Chem. **95**, 7564 (1991)
5. H. Shinohara *et al.*: J. Phys. Chem. **96**, 3571 (1992)
6. K. Kikuchi *et al.*: Chem. Phys. Lett. **216**, 23 (1993)
7. M. Takata *et al.*: Nature **377**, 46 (1995)
8. K. Kikuchi *et al.*: Chem. Phys. Lett. **188**, 177 (1992)
9. S. Iijima: Nature **354**, 56 (1991)
10. S. Iijima, T. Ichihara: Nature **363**, 603 (1993)
11. A. Thess *et al.*: Science **273**, 483 (1996)
12. Y. Yamaguchi, S. Maruyama: Chem. Phys. Lett. **286**, 336 (1998)
13. S. Maruyama, Y. Yamaguchi: Chem. Phys. Lett. **286**, 343 (1998)
14. D.W. Brenner: Phys. Rev. B **42**, 9458 (1990)
15. A.D. Becke: J. Chem. Phys. **98**, 5648 (1993)
16. C. Lee, W. Yang, R.G. Parr: Phys. Rev. B **37**, 785 (1988)
17. M.J. Frisch *et al.*: Gaussian 94 Revision E.1 (Gaussian, Inc., Pittsburgh, PA 1995)
18. E. Curotto *et al.*: J. Chem. Phys. **108**, 729 (1998)
19. S. Nagase *et al.*: Chem. Phys. Lett. **201**, 475 (1993)
20. A. Ayuela *et al.*: Z. Phys. D **41**, 69 (1997)
21. D.L. Strout, B.M. Hall: J. Phys. Chem. **100**, 18 007 (1996)